# Autowaves for Image Processing on a Two-Dimensional CNN Array of Excitable Nonlinear Circuits: Flat and Wrinkled Labyrinths

V. Pérez-Muñuzuri, V. Pérez-Villar, and Leon O. Chua, *Fellow, IEEE*

*Abstract*— **We describe a two-dimensional CNN array of resistively coupled Chua's circuits which can be designed to implement some elementary aspects of spatial recognition, namely, recognizing open curves from closed ones and locating the shortest path between two locations. In the latter, two situations are analyzed: flat and wrinkled surfaces. The two-dimensional CNN array of Chua's circuits is shown, for the first time, to be capable of finding the shortest path between two points on a wrinkled labyrinth. The performance of this parallel processing approach was examined using computer simulations although this method can be implemented in real time via VLSI technology.**

## I. Introduction

BIOLOGICAL systems ordinarily perform reasoning and logical decisions beyond the capabilities of our most sophisticated computer systems. Intuitively, these tasks seem to require mechanisms in which each aspect of the information being processed can act on other aspects, simultaneously influencing and being influenced by them. To implement these mechanisms a class of models called *parallel distributed processing* (PDP) have been developed [1]. These models assume that information processing takes place through the interactions of a large number of simple processing elements called units, each sending excitatory and inhibitory signals to other units.

PDP models are related to *analog neural networks*. Their key features are asynchronous parallel processing, continuous-time dynamics, and global interactions of network elements. In the Hopfield networks [2], [3] each neuron is coupled to every other neuron, thereby rendering it impractical for VLSI realizations.

Cellular neural networks (CNN's) [4], [5] have been developed to overcome this massive interconnection problem. They possess the key features of neural networks, but each unit/cell of the CNN is connected only to its neighbor cells. Each cell contains linear and nonlinear circuit elements. Cells not directly connected together may affect each other indirectly because of the propagation effects of the continuous-time dynamics of the CNN. The CNN can perform parallel signal processing in real time; many examples of its possibilities can be found in the literature [6], e.g., noise removal, corner extraction, edge extraction, connectivity analysis, the Radon transform, thinning, and half-toning.

Recently, Krinsky *et al.* [7], [8] have proposed what they called "the autowave principles for parallel image processing." Autowaves represent a particular class of nonlinear waves, which propagates in an active excitable media at the expense of the energy stored in the medium. The term "autowaves," was coined by R. V. Khokhlov in [9, see Preface] as an abbreviation for "autonomous waves," since such waves can propagate without a forcing function. Autowaves are characteristic of strongly nonlinear active media. They are self-sustained signals that induce a local release of stored energy in an active medium, and use it to trigger the same process in adjacent regions. Typical examples of autowaves include the waves of combustion, of phase transitions, concentration waves in chemical reactions, and also many biological autowave processes (propagation of nerve impulses, excitation waves in the heart muscle, epidemic waves in ecological communities, spreading waves in the cerebral cortex, etc.). These examples stress the importance of the autowave phenomena.

The fundamental properties of autowaves differ basically from those of classical waves in conservative systems. The shape and amplitude of autowaves remain constant during propagation, whereas the amplitude of classical waves attenuates rapidly with the distance and the waveform is distorted by both dispersion and diffusion processes occurring in the medium. Autowaves do not reflect from either the medium boundaries or inhomogeneities. Two colliding autowaves annihilate rather than penetrate one another, and, therefore, no interference takes place. However, both autowaves and classical waves share the property of diffraction. These properties are shared by all the phenomena cited above [10].

Using these properties, Krinsky *et al.* prove the ability of the autowaves for some image processing operations, such as contrast regulation, restoration of a broken contour, and edge detection [7]. Principles of parallel analog information processing by means of distributed systems are also discussed in [11].

In the simplest case, an active medium cannot return to the same state after propagation of an autowave (as for example the case of waves of combustion). Therefore, only one wave can propagate through such a medium. These traveling waves

Manuscript received July 14, 1992; revised October 26, 1992. This work was supported in part by the Office of Naval Research under Grant N00014-89-J-1402 and the National Science Foundation under Grant MIP-8912639.

V. Pérez-Muñuzuri and V. Pérez-Villar are with the Department Física de la Materia Condensada, Facultad de Físicas, 15706, University of Santiago de Compostela, Spain.

L. O. Chua is with the Department of Electrical Engineering and Computer Sciences University of California, Berkeley, CA 94720.

IEEE Log Number 9208126.

can be represented essentially by two states, one is assigned to those parts of the system that are moving along a limit cycle, while the remaining points are represented by the second state. Traveling waves are a particular case of autowaves since they only trigger from one stable equilibrium state to a second one where they remain from then on.

By coupling several Chua's circuits we have been able to show analytically the existence of traveling wave solutions in this system [12], [13]. The diffraction and annihilation of these waves have been found to be extremely interesting properties for image analysis. The purpose of this paper is to show that a two-dimensional CNN array of coupled Chua's circuits can be used for image processing. We will bring to focus some examples, namely, distinction between closed and open curves and finding the shortest path in a labyrinth.

In the last case, two possibilities can appear in real life, since the labyrinth can be flat or wrinkled. For example, the first situation is typical for hospitals or large office buildings where large open surfaces with only walls or furniture blocking the way are common. The second situation could correspond to the case of anyone going from point A to point B separated by some hills with gentle and steep slopes. In this case, the shortest path may not be the one that takes less time since other factors must be considered, for example, the available stored energy. In other words, instead of taking the geometrically shortest path between A and B, which may include climbing steep hills, it may be better to go around the obstacle in order to save energy.

Because our array is a set of resistively coupled Chua's circuits, it has been found that the velocity of the traveling waves decreases with the diffusion coefficient and can fail to propagate at, or below, some critical value of the diffusion coefficient. This phenomenon can be found in a discrete model where the internal dynamics of each circuit cell plays an important role. The distinction between closed and open curves and the finding of the shortest path in a flat labyrinth are well-known examples of image analysis in the literature. But, to the best of our knowledge, we have solved, for the first time, the wrinkled labyrinth problem as a three-dimensional spatial image problem with a two-dimensional nonhomogeneous array of Chua's circuits.

## II. Model of the Two-Dimensional CNN Array of Chua's Circuits

The basic unit (cell) of our two-dimensional CNN array is a Chua's circuit [14]–[19] (Fig. 1), a simple active nonlinear circuit that exhibits a variety of bifurcation and chaotic phenomena. The circuit contains three linear energy-storage elements (an inductor and two capacitors), a linear conductance, and a single nonlinear active resistor. Every cell is coupled to its four closest adjacent neighbors through linear resistors, thereby simulating a diffusion process.

The circuit dynamics for each cell can be described by a third-order autonomous nonlinear differential equation. In particular, we will choose the dimensionless form given by [14, equation (1.1)] [14] which we rewrite for each circuit cell

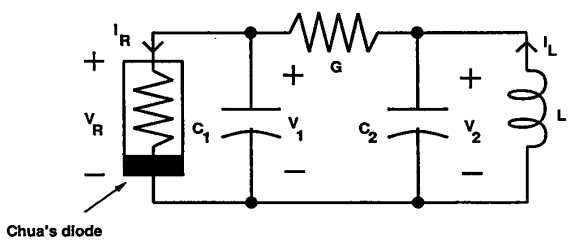


Fig. 1. Chua's circuit consists of a linear inductor $L$, a linear resistor of conductance $G$, two linear capacitors $C_1$ and $C_2$, and a nonlinear resistor known as the Chua's diode. Each unit is connected to its neighbors through linear resistors $R$ at node $V_1$.

at the position $(i, j)$ of the array as

$$\begin{aligned}\dot{x}_{i,j} &= \alpha(y_{i,j} - h(x_{i,j})) \\ &\quad + D[x_{i-1,j} + x_{i+1,j} + x_{i,j-1} + x_{i,j+1} - 4x_{i,j}] \\ \dot{y}_{i,j} &= x_{i,j} - y_{i,j} + z_{i,j} \\ \dot{z}_{i,j} &= -\beta y_{i,j} \end{aligned} \tag{1}$$

where $1 \leq \{i, j\} \leq n$ and $n$ is the size of the array. The function $h(x)$ describes the three- segment piecewise-linear curve of the nonlinear resistor described by

$$\begin{aligned} h(x) &= m_1 x + (m_0 - m_1)x_2 + \epsilon \qquad x \geq x_2 \\ &= m_0 x + \epsilon \qquad x_1 \leq x \leq x_2 \\ &= m_1 x + (m_0 - m_1)x_1 + \epsilon \qquad x \leq x_1 \end{aligned} \tag{2}$$

where $\epsilon$ is a small constant called the "dc offset."

We will choose $x_1 = -1$ and $x_2 = 1$. Observe that in view of the symmetric configuration of the nonlinear characteristics (i.e., its integral is equal to zero), it is necessary to include an offset, $\epsilon \neq 0$, in order to have a traveling wave solution [12].

In (1), $D$ represents the diffusion coefficient of the variable $x$, and is given by

$$D = \frac{\alpha}{GR} \tag{3}$$

in its dimensionless form,[1] where $G$ is the conductance in Siemens of the linear resistor in the Chua's circuit, and $R$ is the coupling resistance in Ohms. $D$ is assumed to be constant in the first two cases presented in this paper. However, a diffusion coefficient which is a function of the position, $D = D(i, j)$, is necessary to describe a wrinkled labyrinth, as we will show later.

The set of fixed parameters used throughout this paper is $\{\alpha, \beta, m_0, m_1\} = \{9, 30, -1/7, 2/7\}$, $G = 0.7$, and $\epsilon = -1/14$. For these values of the parameters the propagation failure mentioned above occurs at, or below, some critical value of the diffusion coefficient $D^* = 0.51 (R^* = 25$ in (3)).

The equilibrium states of (1) obtained by setting $\dot{x}_{i,j} = \dot{y}_{i,j} = \dot{z}_{i,j} = 0$ (for the uncoupled system) are summarized as follows:

| State | $x$ | $y$ | $z$ |
|---|---|---|---|
| $P_+$ | $(m_1 - m_0)/m_1 - \epsilon/m_1$ | 0 | $(m_0 - m_1)/m_1 + \epsilon/m_1$ |
| $P_0$ | $-\epsilon/m_0$ | 0 | $\epsilon/m_0$ |
| $P_-$ | $(m_0 - m_1)/m_1 - \epsilon/m_1$ | 0 | $(m_1 - m_0)/m_1 + \epsilon/m_1$ |

[1] We use the same scaled parameters as in [19].

Here $\boldsymbol{x}$, $\boldsymbol{y}$, and $\boldsymbol{z}$ are vectors of dimension $n \times n$. Each of these three equilibrium states represents a solution to (1) for all values of the parameters. The study of the behavior of the solutions in the neighborhood of the "trivial" equilibrium solutions and the questions of their stability are straightforward, and, in particular, for the Chua's circuit have been described extensively [14]. For the set of parameters given above, the equilibrium states $P_+$ and $P_-$ are stable fixed points, namely, sinks, while the stability of the state $P_0$ depends upon the value of the coupling resistances, $R$. Bifurcation of solution branches from the trivial branch is called "primary bifurcation" in the literature of traveling waves [20], [21]. Only real bifurcations are of interest to us in this paper. Recently, we have shown [12], for the one-dimensional problem, that there is a critical value of the coupling resistance, for a given number of coupled circuits, at which we proved the existence of traveling waves. The simulations shown throughout this paper fulfill this condition. Above this critical value, $P_0$ is a saddle. Thus the interval $(P_-, P_0)$ plays the role of a threshold, exceeding it leads to a transition from the state $P_-$ to state $P_+$.

The nonlinear boundary value problem described by (1) and (2) was completed by imposing zero-flux boundary conditions. A uniform time step of 0.01 was used throughout as the differential equations were integrated using an explicit Euler method. The spatial step size is kept at a constant value equal to one, as a consequence of our assumption of a discrete array.

## III. Examples of Homogeneous Two-Dimensional CNN Array of Chua's Circuits for Image Processing

Here we present two examples for illustrating the possibilities of using a two-dimensional CNN array of Chua's circuits for image processing. Recall that autowaves, and by definition, traveling waves, are not reflected by obstacles and boundaries and do not interfere when two of them collide with each other. Our model is able to recognize open curves and shapes from closed ones, and can identify the shortest path between two locations. Since the autowaves propagate throughout the medium with a *constant* velocity, a large number of circuits operate *simultaneously*. On the other hand, classical methods for detecting closed curves usually consists of scanning all possible points of the array in order to locate first the objective being classified, and then following the boundary of the object, by trial and error, until the closed curve is identified.

For the two examples to be presented below, we make the following assumptions

1) The input image for pattern recognition is "stored into the memory" of our array by *keeping* (i.e., clamping) those circuit cells that coincide with the position of the obstacles, at the same initial state, at all times. This assumption is equivalent, from the point of view of numerical simulation, to imposing some kind of boundary conditions for the obstacles so that traveling waves can surround them because of the diffraction properties of the autowaves.
2) Only binary images are assumed in these two examples. The two allowed states coincide with the two equilibrium states $P_+$ and $P_-$ in Chua's circuits.
3) A traveling wave is always initiated at the left top corner of our array by setting some cells in the Chua's circuits at the positive equilibrium state $P_+$ while maintaining the remaining cells at $P_-$. The traveling wave triggers from $P_-$ to $P_+$ at constant velocity, and spreads throughout the image. We should point out that even though each cell can settle to either $P_\pm$, the state dynamics of each node is continuous (the state of a node is not binary valued).

The pictures presented in this section are obtained by computer simulations with a SUN 4 Workstation. The numerical simulations take 15 minutes to "complete" an array of $45 \times 45$ Chua's circuits.

### 3.1. Detection of Closed Curves

Fig. 2(a) shows two possible obstacles that our model can detect and differentiate. One of them is an open cavity (left top of the figure) while the second one is a closed obstacle.

The set of computer snapshots in Fig. 2 shows the traveling wave propagating throughout the input image. Because of the dispersion (with neither interference nor reflection) property of autowaves, the traveling wave surrounds the wall of the open cavity and differentiates the closed obstacle by bypassing it, from those that are opened by filling up the open space. Thus, the closed objects will remain at the initial state $P_-$. This criterion can distinguish a closed curve from an unclosed one.

This method can be implemented by adding a simple decision circuit designed to identify the cells that have triggered from a negative initial state to a positive final state. Another possibility is to generate the difference picture of the result of this transformation from the original image. Then, the closed curves can be detected. Observe that unlike many other approaches, this method for closure detection is *invariant against translation, rotation, and scaling.*

This application of autowaves for image processing can also be implemented by a CNN cloning template [27].

### 3.2. Shortest Path in a Flat Labyrinth

This application follows from the first example. After a traveling wave is initiated at the left top corner of Fig. 3(a), it propagates throughout the image (see consecutive snapshots Fig. 3(b) to (f). Because of its *constant velocity*, the shortest path will coincide with the path that takes the least time. Let us suppose that our wave must find the shortest path to reach the left bottom corner of the image. In this case, our autowave "explores" all the possible ways to reach that point. In the successive snapshots shown in Fig. 3, observe that upon hitting the obstacle, centered at cell (17, 26), the traveling wave splits and eventually surrounds this object (Fig. 3(d)), and finally annihilates each other when the two wave fronts collided with each other [7].

Fig. 3(f) shows the final state when the program stops after the wave reaches the left bottom corner.

## IV. The Wrinkled Labyrinth

In this case, a new third degree of freedom is added to our problem. Suppose the ground is not flat but wrinkled. In this

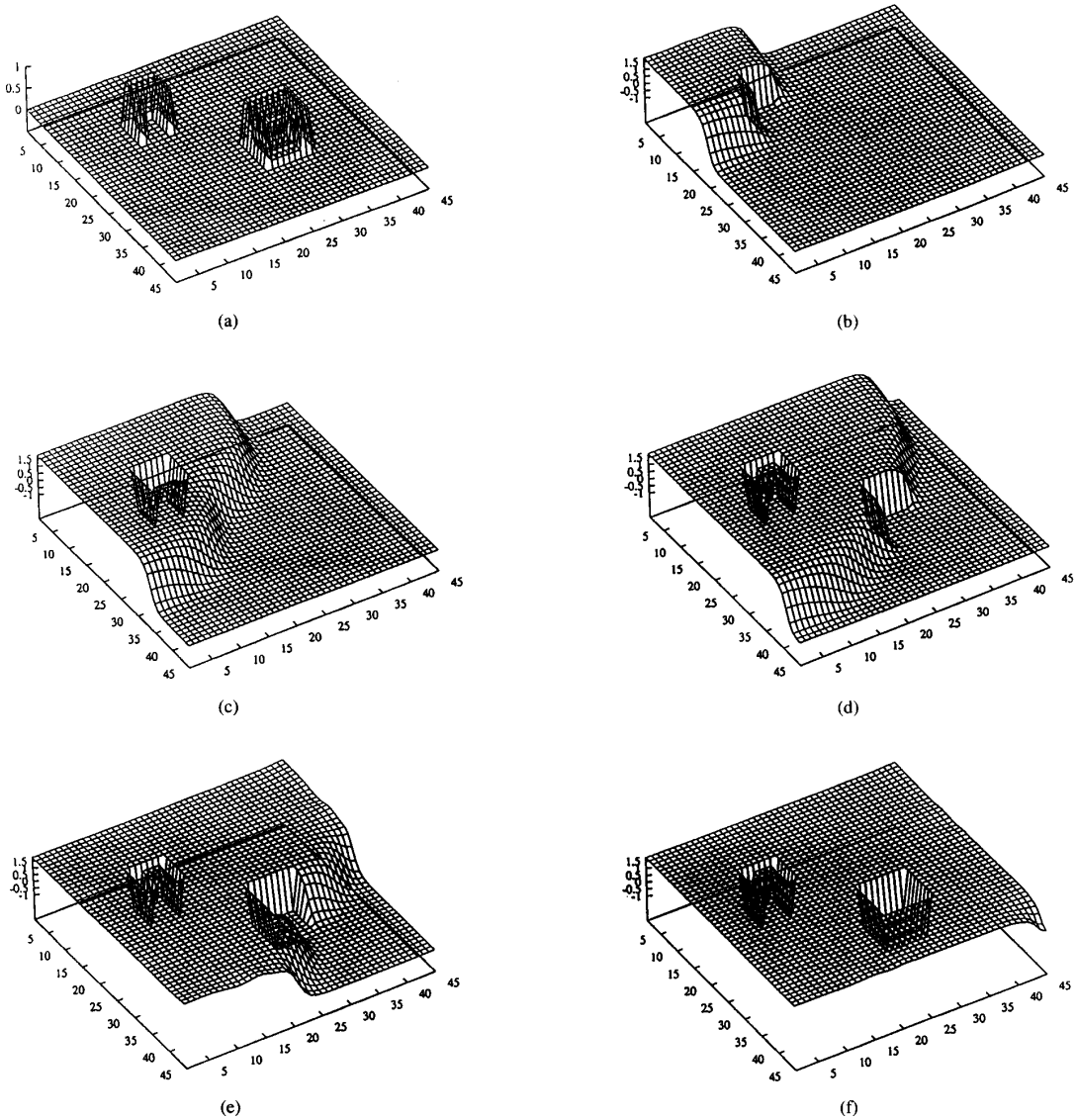

Fig. 2. (a) The input image; a cavity and an obstacle on a 45 × 45 CNN array of Chua's circuits. (b)–(f): the traveling wave initiated at the top left cell (1, 1) of the figure spreads throughout the image surrounding the obstacles and enters the cavity. In this way, both objects are identified.

case, the shortest path is the path that takes the least energy. This class of problems could be useful for moving systems with a limited amount of stored energy between two points on an undulated surface.

From a numerical point of view, this situation can be achieved with a discretized array of cells, each one connected to their adjacent neighbors through *different* linear resistors $R$. These resistors, which vary from $R_{\min}$ to $R_{\max}$ are used to code the difficulty of the slopes. Gentle slopes will correspond to values of $R$ which are close to $R_{\min}$, while steep slopes correspond to values of $R$ close to $R_{\max}$. This code can distinguish whether the wave is climbing upward on downward between two cells by assigning two different values of the resistance depending upon the direction of the traveling wave propagation.

Then, the input image is a black and white photo with different tonalities of greys of the wrinkled terrain where for example, the clearest parts of the photo correspond to the higher zones of the terrain and are therefore identified with $R_{\max}$. The remaining tonalities are identified with corresponding values of resistors until the minimum allowed value, $R_{\min}$, is reached. This can be achieved experimentally by fixing the value of the coupling linear resistors with voltage-controlled resistances [28], [29]. Thus, the different grey tonalities are discretized into discrete voltages levels.

As mentioned in the Introduction, the discretized version

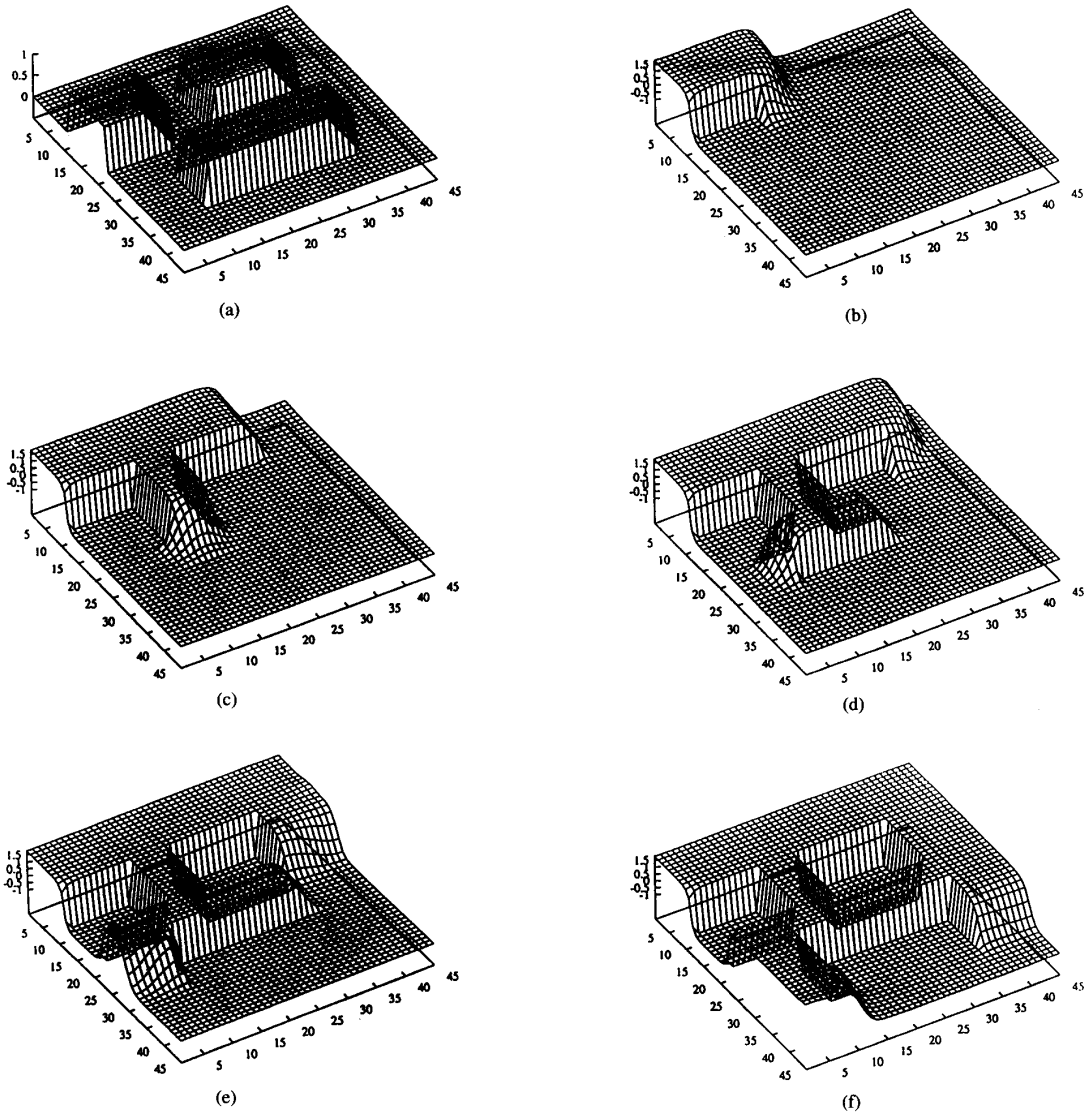


Fig. 3. (a) The input image; a labyrinth defined by three obstacles on a two-dimensional array of Chua's circuits (b)–(f) the traveling wave initiated at the top left cell (1, 1) of the input image spreads throughout the image. The autowave properties of annihilation and diffraction are clearly seen. The traveling wave stops when it reaches the final cell (45, 45), left bottom of the figure.

of the coupled Chua's circuits exhibits an interesting effect usually found in nerve propagation, namely, "propagation failure." By choosing those points of the terrain that are unreachable for our autowave to values of $R$ at, or greater than, some critical value $R^*$ where the "failure" phenomenon appears, the traveling wave propagating throughout the array will fail to propagate from those points that remain isolated from the rest of the image.

Fig. 4(a) represents a possible undulated terrain. This image shows the discretized values of the resistance for the interval, $1 < R < 30$. The cell located near the top of the *Mexican hat* is assumed to be unreachable for the autowave and hence, its coupling resistances have been set to values of $R \geq R^* = 25$. The objective is to find the best path between the top cell (1, 1) and the bottom-corner cell (45, 45) of Fig. 4(a). As in the preceding examples, the image processing begins when a traveling wave is initiated at the top cell (1, 1) of Fig. 4(a) by setting the cell (1, 1) at the steady state $P_+$ at $t = 0$, while the remaining cells are set at $P_-$. After that ($t > 0$), the autowave spreads throughout the wrinkled labyrinth, as expected.

Obviously, for the homogeneous case, the shortest path is along the diagonal of the array. In this case, in view of the inaccessibility of the top of the Mexican hat, the autowave finds the best path by flowing and engulfing around the obstacle. The set of Fig. 4(b)–(f) shows this behavior. In those zones of the array where the coupling resistance is close to the critical value $R^*$, the autowave velocity decreases, while in the other favorable zones (gentle slopes) its velocity increases.

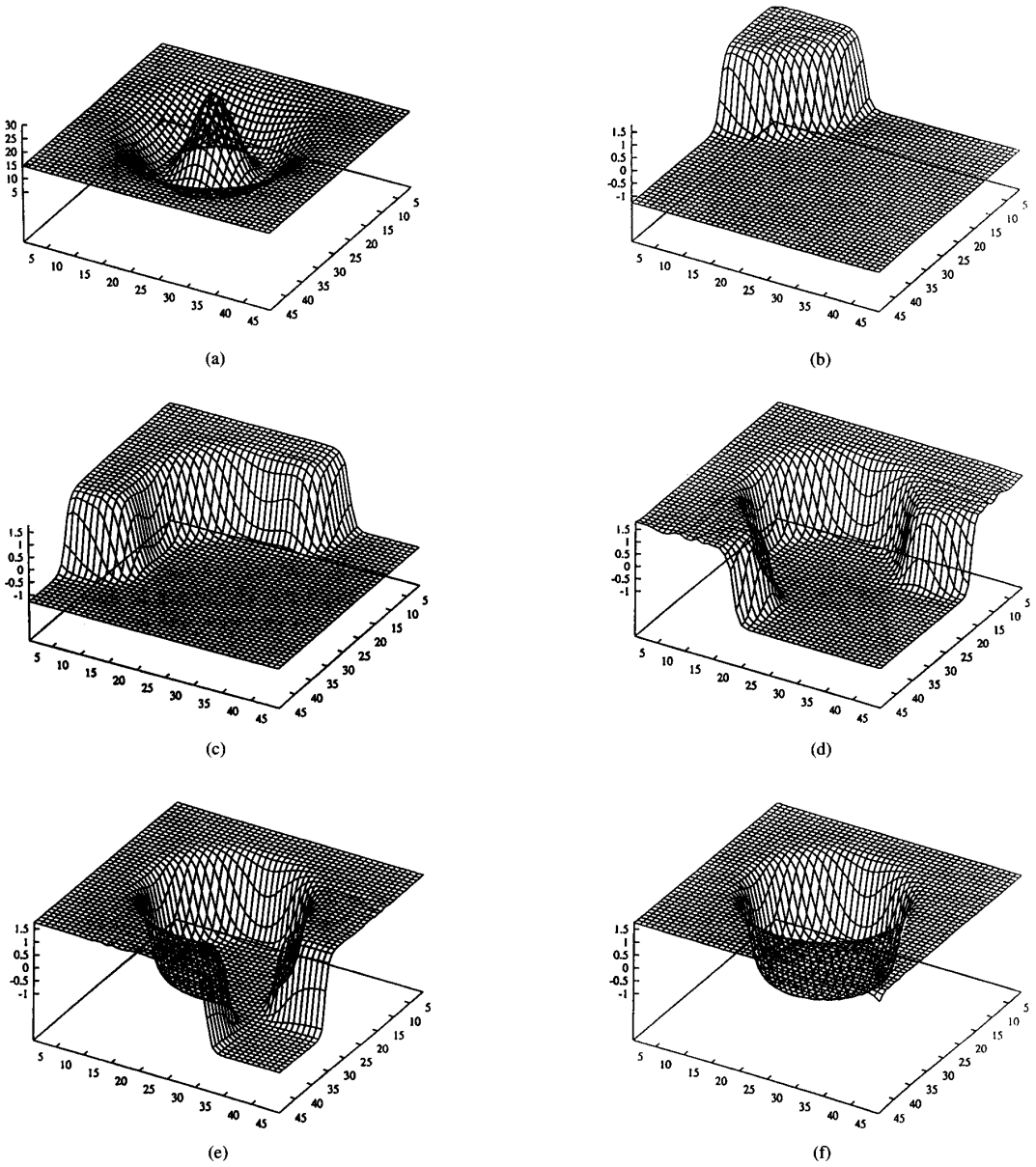


Fig. 4. The wrinkled labyrinth. In this case, a new third degree of freedom is added to our problem; the ground is not flat but wrinkled. In this case, the shortest path is the path that takes the least energy. (a) The input image; a Mexican hat. This image shows the discretized values of the resistance in the interval, $I < R < 30$ (the diffusion coefficient, (3), is a function of the position). (b)–(f); the traveling wave initiated at the top of the figure (a) spreads throughout the image. (f) shows the final state when the autowave reaches its destination. The hole at the center of the picture represents those places where the autowave can not reach. The shortest path or the path that takes the least time surrounds the pick of the hat.

Once the autowave reaches our destination cell (45, 45) at the bottom corner; it stops to propagate (Fig. 4(f)).

This approach allows us to save the system's stored energy by choosing the most favored path, i.e., the path where the diffusion processes involved in the wave propagation are favored.

## V. Finding the Shortest Path

Algorithms for finding the shortest path between two points have been widely studied in the literature [22]–[26]. Explicitly, the "search and trace algorithms" described by Lee in [24] can be applied herewith. On the other hand, the flat case could correspond to the simple all-symbol mapping and the wrinkled case to the complex cell-symbol mapping routing models [24]. Nevertheless, the task of finding the shortest path is not evident at all. We have used simple algorithms to find it.

1) With the help of a simple external circuit, the times at

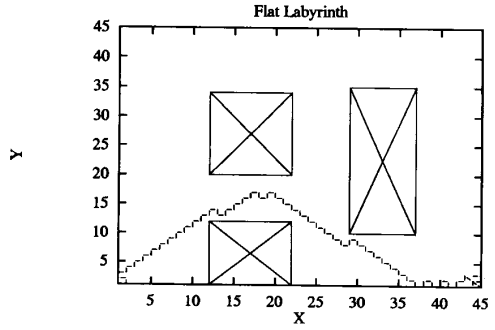


Fig. 5. Shortest path found for the flat (Fig. 3) labyrinth. The traveling wave was initiated at cell (1, 1) and it stops at cell (45, 1). The crossed squares in Fig. 5(a) corresponds to the obstacles defined in Fig. 3(a). Our results are equivalent to those already found by Lee [24], but the optimum path can be found much faster because of the highly parallel processing of the autowave method.

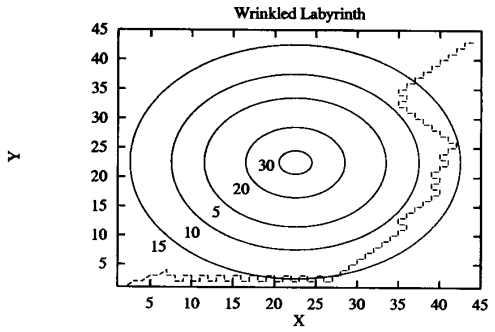


Fig. 6. Shortest path for the wrinkled (Fig. 4) labyrinth. As in Fig. 5 the traveling wave was initiated at cell (1, 1) and it stops at cell (45, 45). The contours show the different surface levels (different values of the coupling resistance (Fig. 4(a)) indicated by the numbers close to each contour). From the outside to the inside of the graph, the values of the resistance change continuously from 15 to 5, then increases to the value 30, at the top of the hill. Note that the traveling wave finds the shortest path by surrounding the pick of the *Mexican hat* and then going down the valley and coming back to the neighborhood of the hill.

which the cells had triggered from state $P_-$ to $P_+$ can be stored and compared in order to determine the path that takes the least time to reach the final destination.

2) In the case where several cells have triggered from state $P_-$ to $P_+$ at the same time, then the cell that is closer to the last point but farther from the first point is added to the list of cells defining the shortest path. It is possible to show that this is equivalent to storing the direction of wave propagation at each cell, i.e., which neighbor cell contributes more to the diffusion process during the propagation. In other words, what signals converged onto a cell before excitation.

We have applied the above algorithms to find the shortest path for the flat and wrinkled labyrinths (Figs. 5 and 6). For the flat labyrinth we have reproduced the results already found by Lee [24]. On the other hand, in our case, the autowave method improves the processing of the image, since all elements of the medium evolve their states simultaneously, resulting in a very high degree of parallelism.

Fig. 6 shows the shortest path found for the wrinkled labyrinth. The contours correspond to the main surface levels (different values of the coupling resistance (Fig.4(a)), indicated by the numbers next to each contour). Observe that the traveling wave finds the shortest path to arrive at cell (45, 45) by going around the *Mexican hat*, down the valley, and then coming back to the neighborhood of the pick. Because of the different values of the coupling resistances, the traveling wave naturally chooses those points where its velocity can be increased in order to take the least time to achieve its objective.

## VI. Conclusions

We have shown that a two-dimensional CNN array of Chua's circuits can be used for image analysis. Results similar to those proposed by Krinsky *et al.* [7] for autowave propagation have been reproduced numerically, namely, detection of closed curves and finding the shortest path in a labyrinth. On the other hand, we have shown for the first time, how it can be applied to a CNN array of excitable nonlinear circuits for the shortest path in a wrinkled labyrinth.

In a resistively coupled homogeneous array of Chua's circuits, a traveling wave will propagate throughout the input image. Obviously, the examples shown in Section III are a special case of the wrinkled labyrinth. By using a nonhomogeneous array it is possible to analyze three-dimensional surfaces, or undulated surfaces, in order to find the *best path* (i.e., the one that favors the autowave propagation) between two points. The unreachable places for our autowave can be fixed by setting the corresponding cells of the CNN array to be coupled to their neighbors through resistances at, or greater values than $R^*$. Since for $R \geq R^*$ the wave fails to propagate [12], [13], these points of the input image will remain isolated from the rest, as if they were obstacles.

It is important to remark that for autowave processes the traveling wave velocity, $v$, scale as

$$v \cong \gamma \sqrt{\frac{R^* - R}{RR^*}} \tag{4}$$

i.e., for values of the resistance lower than $R^*$ and close to the allowed $R_{\min}$ the changes in the values of the velocity are small if we compare with $R$. Consequently, for the wrinkled labyrinth shown in Fig. 4(a), our autowave cannot identify perfectly the best path, which corresponds to going through the lower values of resistance in Fig. 4(a). To solve this problem the input image can be discretized for values of the resistance closer to $R^*$. In this case, the ability of the autowave to identify the best path is improved, but the process becomes slower.

Simple algorithms have been proposed in order to solve the shortest path problem. Those algorithms are equivalent to those proposed by Lee [24]. Nevertheless a more powerful path algorithm must be developed for all cases, independent of the degree of wrinkles of the surface or the chosen values for $R_{\max}$ and $R_{\min}$.

The wrinkled labyrinth is a powerful technique to discriminate steep slopes from gentle slopes, as well as to indicate to an autonomous system in real time which places are unreachable, depending on its stored energy. This technique is based on

the observation that the state of each cell can be changed in order to vary the value of the critical resistance $R^*$ via some external controlling parameters [13].

The possibility of building large arrays of Chua's circuits via VLSI technology, as well as the use of voltage-controlled resistors to store the undulated surfaces, make this autowave approach a unique tool for real time image processing.

## ACKNOWLEDGMENT

The authors want to thank Profs. V. I. Krinsky, J. L. F. Porteiro, and Tibor Kozek for helpful discussions.

## REFERENCES

[1] J. L. McClelland and D. E. Rumelhart, *Parallel Distributed Processing.* Cambridge, MA: MIT Press, 1988.
[2] J. J. Hopfield. "Neural networks and physical systems with emergent computational abilities," in *Proc. Nat. Acad. Sci. USA*, vol. 79, 1982, pp. 2554–2558, and "Neurons with graded response have collective computational properties like those two-state neurons," *Proc. Nat. Acad. Sci. USA*, vol. 81, 1984, pp. 3088–3092.
[3] J. J. Hopfield and D. W. Tank, "Computing with neural circuits: A model," *Science*, vol. 233, pp. 625–633, 1986.
[4] L. O. Chua and L. Yang, "Cellular neural networks theory," *IEEE Trans. Circuits Syst.*, vol. 35, pp. 1257–1272, 1988.
[5] ——, "Cellular neural networks: Applications," *IEEE Trans. Circuits Syst.*, vol. 35, pp. 1273–1290, 1988.
[6] L. O. Chua, L. Yang, and K. R. Krieg, "Signal processing using cellular neural networks," *J. VLSI Signal Processing*, vol. 3, pp. 25–51, 1991.
[7] V. I. Krinsky, V. N. Biktashev, and I. R. Efimov, "Autowaves principles for parallel image processing," *Physica 49D*, pp. 247–253, 1991.
[8] L. Kunhert, K. I. Agladze, and V. I. Krinsky, "Image processing using light-sensitive chemical waves," *Nature*, vol. 337, pp. 244–247, 1989.
[9] M. T. Grekhova, "Autowave processes in systems with diffusion," *Gorky*, Acad. Sci. USSR, 1981.
[10] V. I. Krinsky, "Autowaves: Results, problems, outlooks" in *Self-Organization: Autowaves and Structures far from Equilibrium*, V. I. Krinsky, Ed. New York: Springer-Verlag, pp. 9–19, 1984.
[11] A. S. Mikhailov, "Engineering of dynamical systems for pattern recognition and information processing," in *Nonlinear Waves 2*, A. V. Gaponov-Grekhov, M. I. Rabinovich, and J. Engelbrecht, Eds. New York: Springer-Verlag, pp. 104–115, 1989.
[12] V. Pérez-Muñuzuri, V. Pérez-Villar, and L. O. Chua, "Traveling wave front and its failure in a one-dimensional array of Chua's circuits," (Special Issue of Chua's Circuit: A paradigm for chaos.)*J. Circuits Syst. Comp.*, vol. 3, pp. 215–229, Mar. 1993.
[13] ——, "Propagation failure in linear arrays of Chua's circuits," *Int. J. Bif. and Chaos*, vol. 2, pp. 403–406, 1992.
[14] L. O. Chua, M. Komuro, and T. Matsumoto, "The Double Scroll family—Parts I and II," *IEEE Trans. Circuits Syst.*, vol. CAS-33, pp. 1073–1118, 1986.
[15] J. Cruz and L. O. Chua, "A CMOS IC nonlinear resistor for Chua's circuit," *IEEE Trans. Circuits Syst.*, vol. 39, pp. 985–995, Dec. 1992.
[16] L. O. Chua, Global unfolding of Chua's circuit," *IEICE Trans. on Fundament. of Electron., Commun., Comp. Sci.*, vol. E76A, May 1993.
[17] M. P. Kennedy, "Robust op amp realization of Chua's circuit," *Frequenz.*, vol. 46, pp. 66–80, 1992.
[18] L. O. Chua, "The genesis of Chua's circuit," *Arch. Elek. Ubertragung.*, vol. 46, pp. 230–257, 1992.
[19] T. Matsumoto, L. O. Chua, and M. Komuro, "The double scroll," *IEEE Trans. Circuits Syst.*, vol. CAS-32, pp. 797–818, 1985.
[20] T. J. Mahar and B. J. Matkowsky, "A model biochemical reaction exhibiting secondary bifurcation," *SIAM J. Appl. Math.*, vol. 32, pp. 394–404, 1977.
[21] M. Kubicek and M. Marek, *Computational Methods in Bifurcation Theory and Dissipative Structures.* New York: Springer-Verlag, 1983.
[22] G. B. Dantzig, "Maximization of a linear function of variables subject to linear inequalities," Cowles Commission, 1951.
[23] L. R. Ford and D. R. Fulkerson, "Maximal flow through a network," *Can. J. Math.*, vol. 8, pp. 399–404, 1956.
[24] C. Y. Lee, "An algorithm for path connections and its applications," *IRE Trans. Electron. Comp.*, vol. EC-10, pp. 346–365, 1961.
[25] E. F. Moore, "Shortest path through a maze," in *Ann. Computation Lab. of Harvard Univ.*, Cambridge, MA: Harvard University Press, vol. 30, pp. 285–292, 1959.
[26] R. C. Prim, "Shortest connection networks and some generalizations," *Bell Syst. Tech. J.*, vol. 36, pp. 1389–1401, 1957.
[27] T. Matsumoto, L. O. Chua, and R. Furukawa, "CNN cloning template: hole-filler," *IEEE Trans. Circuits Syst.*, vol. 37, pp. 635–638, 1990.
[28] R. Senani and D. R. Bhaskar, "Realization of voltage-controlled impedances," *IEEE Trans. Circuits Syst.*, vol. 38, pp. 1081–1086, 1991.
[29] K. W. Nay and A. Budak, "A voltage-controlled-resistance with wide dynamic range and low distortion," *IEEE Trans. Circuits Syst.*, vol. 30, pp. 770–772, 1983.

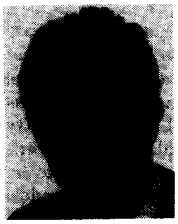

**Vicente Pérez Muñuzuri** received the Physics degree and Doctor in Physics degree from the University of Santiago de Compostela, Spain, in 1988 and 1992, respectively.

From 1988 to 1990, he was a visiting scholar at the C.N.R.S. Paul Pascal, Bordeaux, France. Since 1991, he has been with the Department of Fisica de la Materia Condensada of the University of Santiago de Compostela. His research interests include chaos and bifurcation theory, pattern formation, and nonlinear dynamics.

Dr. Pérez Muñuzuri is a member of the American Mathematical Society.

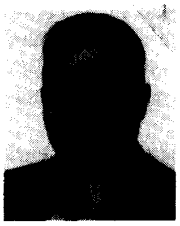

**Vicente Pérez Villar** received the Science degree and Doctor in Physics degree from the University of Seville in 1962 and 1966, respectively, and the Diplome d'etudes superiores de sciences physiques from the University of Clermont Ferand, France.

From 1963 to 1968, he was Assistant and Professor Adjunto at the Department of Termodinamica of the University of Seville. From 1968 to 1973, he was Professor Catedratico at the Department of Fisica Fundamental, University of Valladolid, Spain. Since 1973, he has been with the Department of Materia Condensada of the University of Santiago de Compostela, Spain, as Professor Catedratico. In 1988, he was elected Dean of the Facultad de Fisicas. His research interests are in the areas of nonlinear dynamics and pattern formation. He is the author of numerous papers.

Dr. Pérez Villar is a member of the Real Sociedad Espanola de Fisica, Societe Francaise de Chimie, and the European Physical Society.

**Leon O. Chua** (S'60–M'62–SM'70–F'74), for a photograph and biography please see page **156** of this issue.